

Hafnium Chloride Cluster Chemistry. An Exploration

Ru-Yi Qi and John D. Corbett*

Department of Chemistry, Iowa State University, Ames, Iowa 50011

Received June 14, 1994[®]

Many Hf–HfCl₄–Z systems have been explored to establish the stability and structures of Hf₆(Z)Cl₁₂Cl_n cluster phases relative to the large variety known for zirconium. The slowness of Hf–HfCl₄ reactions and the limited number of new phases required special care in synthesis to avoid excessive HfCl₄ pressures. Only B and C interstitials (Z) gave cluster phases, namely (1) AHf₆Cl₁₄Z with A = Li, Na, K, or nothing and Z = B or C, in stuffed versions of the orthorhombic Nb₆Cl₁₄ structure; (2) orthorhombic AHf₆Cl₁₅C with A = K or Cs separately occupying one of the two different cation lattice sites in the CsKZr₆Cl₁₅B structure type; (3) cubic Na_{~0.8}Hf₆Cl₁₅B (stuffed Ta₆Cl₁₅) plus Na_{0.8}Hf₆Cl₁₅B in a tetragonal subgroup when prepared with more sodium. The Na_{1.0}Zr₆Cl₁₅B analogue of the last was also prepared and structurally refined [Na_{0.8(2)}Hf₆Cl₁₅B, *Ia* $\bar{3}$ d, Z = 16, *a* = 21.428(2) Å, *R/R_w* = 5.3/4.3%; Na_{0.76(6)}Hf₆Cl₁₅B, Na_{1.04(5)}Zr₆Cl₁₅B, *I4*₁*acd*, Z = 16, *a* = 21.540(2), 21.622(2) Å, *c* = 21.387(3), 21.793(3) Å, *R/R_w* = 5.5/4.1, 5.6/5.4%, respectively]. The tetragonal distortions in the last are in the opposite sense (*c/a* = 0.9929 for Hf, 1.0079 for Zr). Both distortions from cubic seem to give smaller clusters, slightly longer M–Cl^{*a*} distances, and an additional secondary chlorine neighbor about one of the split, fractional sodium positions. Volumes of hafnium cluster phases are 1.6–2.9% smaller than those of the analogous zirconium compounds and, in one comparable case, *d*(M–B) is ~0.03 Å less for Hf than for Zr.

Introduction

Extensive investigations of reduced halides of zirconium and of the group 3 transition metals over the past decade have revealed a rich cluster chemistry. A common theme throughout has been the necessity of a centered interstitial atom in each cluster. Among these, the zirconium chloride and iodide systems are the most systematically studied and the best understood. The substantial variety of compositions and structures achieved fall largely in the series A_{*m*}[Zr₆X₁₂Z]X_{*n*}, where A = an alkali, alkaline-earth or rare-earth metal; X = Cl, Br, or I, and 0 ≤ *n*, *m* ≤ 6, while Z may come from a wide range of main-group or transition-metal elements. The chlorides afford the largest and most complete group in this category,^{1–6} while the iodides, though more limited in *n*, *m* values, bind a greater range of Z.^{7–9} The bromides form a surprising number of phases and structures that are unknown with either chloride or iodide.¹⁰

The halide cluster chemistry of transition elements that neighbor zirconium is quite varied. Besides the traditional cluster examples of niobium and tantalum,¹¹ the rare-earth-metal iodides (and a few bromides) show a distinctive and diverse chemistry that includes both discrete and condensed cluster examples, and these may encapsulate an even wider interstitial variety.^{12–14} Titanium has so far shown an analogous chemistry

only in Ti₆Cl₁₄C, which was synthesized by a metallocyclic reaction at a relatively low temperature.¹⁵ Unlike the zirconium halide examples, the thermodynamic products obtained from reduced titanium halide systems at higher temperatures have been phases like KTi₄Cl₁₁, CsTi₂Cl₇, and CsTi₄Cl₁₁ which exhibit, at most, only triangular metal clusters.^{16–18}

The present article reports the results of an extensive investigation of the analogous hafnium chloride systems which has revealed only a limited number of cluster parallels.

Experimental Section

Materials. The hafnium employed in this research was a crystal bar product from Teledyne-Wah Chang, with reported analyses in ppm (wt) of Zr 129, Ta < 100, Nb, Fe, O < 50, C < 30, all others < 25 ppm. This Zr content corresponds to 0.023 at.%. We were not able to detect zirconium by SEM-EDX means. Hafnium powder was prepared via the hydrogenation–dehydrogenation method commonly used in this group.⁵ Cold-rolled Hf sheets were cleaned with a mixed acid solution (45% concentrated HNO₃, 10% concentrated HF, 45% H₂O by volume), thoroughly rinsed with water, and dried in air. About 10 g of strips were typically placed in a Mo boat within a fused silica container, and this was evacuated and purged with hydrogen (Matheson, 99.999%) at least three times before being heated to 500 °C. Following an initially rapid hydrogen uptake, the sample was gradually heated to about 550–600 °C and then cooled under hydrogen. The hydride was ground with a diamond mortar and pestle within a N₂-filled glovebox (<1 ppm (vol) H₂O) until the powder passed through an 150-mesh sieve. This HF_x powder was then reloaded into the Mo boat and dehydrogenated by slowly heating under dynamic vacuum (10^{–5} Torr) from 200 to 700 °C, after which the hafnium was reground to pass the same sieve. The refined lattice constants of Hf from Guinier powder data at ~20 °C were *a* = 3.1949(2) Å, *c* = 5.0551(4) Å (*V* = 44.686–(6) Å³), reasonably close to those reported by Romans et al.,¹⁹ *a* = 3.198 Å, *c* = 5.061 Å, considering that their crystal bar Hf contained 1.5 (presumably wt)% Zr.

[®] Abstract published in *Advance ACS Abstracts*, November 15, 1994.

- (1) Ziebarth, R. P.; Corbett, J. D. *Acc. Chem. Res.* **1989**, *22*, 256.
- (2) Zhang, J.; Corbett, J. D. *J. Less-Common Met.* **1989**, *156*, 49.
- (3) Zhang, J.; Ziebarth, R. P.; Corbett, J. D. *Inorg. Chem.* **1992**, *31*, 614.
- (4) Zhang, J.; Corbett, J. D. *Inorg. Chem.* **1991**, *30*, 431.
- (5) Zhang, J.; Corbett, J. D. *Inorg. Chem.* **1993**, *32*, 1566.
- (6) Zhang, J.; Corbett, J. D. *J. Solid State Chem.* **1994**, *109*, 265.
- (7) Rosenthal, G.; Corbett, J. D. *Inorg. Chem.* **1988**, *27*, 53.
- (8) Smith, J. D.; Corbett, J. D. *J. Am. Chem. Soc.* **1986**, *108*, 1927.
- (9) Hughbanks, T.; Rosenthal, G.; Corbett, J. D. *J. Am. Chem. Soc.* **1988**, *110*, 1511.
- (10) Qi, R.-Y.; Corbett, J. D., to be published.
- (11) Wells, A. F. *Structural Inorganic Chemistry*, 5th ed.; Clarendon Press: Oxford, UK, 1984; p 432.
- (12) Payne, M. W.; Corbett, J. D. *Inorg. Chem.* **1990**, *29*, 2246.
- (13) Park, Y.; Corbett, J. D. *Inorg. Chem.* **1994**, *33*, 1705.
- (14) Llusar, R.; Corbett, J. D. *Inorg. Chem.* **1994**, *33*, 849.

(15) Hinz, D. J.; Meyer, G. *J. Chem. Soc., Chem. Commun.* **1994**, 125.

(16) (a) Schäfer, H.; Laumann, R. *Z. Anorg. Allg. Chem.* **1981**, *474*, 135.

(b) Krebs, B.; Henkel, G. *Z. Anorg. Allg. Chem.* **1981**, *474*, 149.

(17) Zhang, J.; Corbett, J. D. *Z. Anorg. Allg. Chem.* **1990**, *580*, 3.

(18) Zhang, J.; Qi, R.-Y.; Corbett, J. D. *Inorg. Chem.* **1991**, *30*, 4794.

(19) Romans, P. A.; Paasche, O. G.; Kato, H. *J. Less-Common Met.* **1965**, *8*, 23.

HfCl₄ was synthesized by the direct reaction of the elements in an evacuated and sealed, two-armed fused-silica vessel. Liquid Cl₂ (>99.5%, Matheson) was maintained at -30 to -40 °C in a trap at one end with the aid of a saturated CaCl₂/ice bath, while the other end, which contained a slight excess of hafnium strips, was heated with a gas torch to initiate the reaction. Once ignited, the reaction proceeded spontaneously; however, periodic heating with the torch, especially near the completion of the reaction, was necessary to maintain a reasonable rate and to prevent blockage of the reaction arm by crude HfCl₄. The raw HfCl₄ was purified by multiple sublimations over hafnium metal and through a glass frit under dynamic vacuum. The sublimed HfCl₄ was colorless and poorly crystalline.

Reagent-grade alkali-metal chlorides were dried under dynamic vacuum below 200 °C and then sublimed. All the starting materials were stored either in sealed ampoules or divided into small portions and kept in stoppered vials that were stored in jars in the glovebox. Amorphous B (Aldrich, 99.999%), small Be chunks (Aldrich, 99.9%), and graphite (National brand, spectroscopic grade, Union Carbide) were introduced into the syntheses as the elements.

Reaction Techniques. As for zirconium halide reactions, all hafnium chloride reactions were carried out in welded Ta tubing in turn encased in fused silica jackets that had been well-evacuated and then sealed. A 200 mg scale was typical. Temperatures around 750–850 °C were used; higher values usually resulted in cluster decomposition. In accord with our earlier studies of HfCl₄,²⁰ Hf–HfCl₄ reaction rates are extremely low relative to those of zirconium, and respectable yields were obtained in the present work only at 600 °C and above and after considerable reaction periods. The high pressures generated by liquid HfCl₄ (subl pt ~320 °C) and HfCl₃ either in the early stages of a reaction or, especially, throughout unsuccessful synthetic attempts often caused the Ta tubing to distend at the crimps or even to leak at the weld. (We have never observed the latter to occur explosively.) Special precautions were therefore taken to prevent any explosion of the silica jacket caused by the high internal pressures following Ta container leakage. Reactions were first heated slowly up to 500 °C and kept at this temperature for 1 or 2 days to allow some reduction of the HfCl₄. The degree of bulging of the crimps at the welded ends of the tubing was checked before the temperature was increased further. In addition, one end of the furnace was elevated, and a small portion of the silica jacket was allowed to extend outside the furnace at the lower end to allow for condensation of HfCl₄ should the Ta container fail. Not surprisingly, the yields of polycrystalline phases containing reduced hafnium chloride clusters were often in the range of only 30–50% after periods of 4 weeks, nonreduced ternary phases (not isostructural with A₂ZrCl₆), and HfCl_x making up much of the remainder. High yields (85–90%) could be realized in favorable cases only if extended reaction periods, e.g., 2–3 months, were utilized. The passivity of Hf metal appeared to be the primary problem; alkali-metal chlorides, AlCl₃ or Hg₂Cl₂ did not materially change yields. Interstitial transport was not a problem judging from the other phases formed, including HfC.

X-ray Studies. Guinier powder diffraction with Cu Kα₁ radiation utilizing an Enraf-Nonius unit was routinely carried out on the products of every reaction to characterize the results, to estimate the relative yields, and, if necessary, to obtain lattice parameters by least squares techniques. Powdered Si (from NIST) was used as an internal standard. The quality of potential single crystals was always checked by oscillation or Laue photos on a Weissenberg camera prior to data collection. If possible, Weissenberg films of more than one layer were also obtained to provide information on cell dimensions, lattice symmetry, and extinction conditions. In some cases, Weissenberg films were taken after a structure had been solved in order to verify the absence of possible superstructures or to confirm certain extinction conditions.

All diffraction data collections were performed at ambient temperature to 2θ = 50° on either a Rigaku AFC6R (rotating anode) or an Enraf Nonius CAD4 diffractometer equipped with a graphite monochromator to give clean Mo Kα radiation (λ = 0.710 73 Å). For each data set, three intense reflections were used as standards to monitor any possible decay or instrument instability. Following each data

Table 1. Selected Crystal and Refinement Data

	Na _{0.8(2)} Hf ₆ Cl ₁₅ B	Na _{0.76(6)} Hf ₆ Cl ₁₅ B	Na _{1.04(5)} Zr ₆ Cl ₁₅ B
space group, <i>Z</i>	<i>Ia</i> 3̄ <i>d</i> (no. 230), 16	<i>I</i> 4 ₁ / <i>acd</i> (no. 142), 16	<i>I</i> 4 ₁ / <i>acd</i> (no. 142), 16
cell parameters ^a			
<i>a</i> (Å)	21.428(2)	21.540(2)	21.622(2)
<i>c</i>		21.387(3)	21.793(3)
fw, ρ _{calc} (g cm ⁻³)	1632, 4.407	1631, 4.367	1114, 2.905
abs coeff (Mo Kα, cm ⁻¹)	267.8	264.3	39.48
transm coeff range	0.78–1.00	0.35–1.00	0.77–1.00
<i>R</i> , ^b %	5.3	5.5	5.6
<i>R</i> _w , ^c %	4.3	4.1	5.4

^a Guinier data, 22 °C, λ = 1.540 562 Å. ^b $R = \sum ||F_o| - |F_c|| / \sum |F_o|$. ^c $R_w = [\sum w(|F_o| - |F_c|)^2 / \sum w(F_o)^2]^{1/2}$, $w = \sigma_F^{-2}$.

collection, ψ -scans at intervals of 10° in ϕ were collected for at least three intense reflections near $\chi = \pm 90^\circ$ for the purpose of an empirical absorption correction. Refined unit cell parameters from Guinier powder data were employed in all cases in the calculation of bond distances and angles as these have higher accuracy than those typically obtained with the aid of single crystal diffractometers. Selected data on the single crystal studies are given in Table 1. More information along with anisotropic displacement results are contained in the supplementary material, and these along with structure factor data are available from J.D.C.

Syntheses and Single Crystal Studies. Cubic Na_{0.8}Hf₆Cl₁₅. This phase was originally observed in ~40% yield after reactions loaded as NaHf₆Cl₁₄B and NaHf₆Cl₁₅B had been carried out at 850 °C for 30 days. A subsequent reaction loaded with the indicated Na_{0.8}Hf₆Cl₁₅B stoichiometry (below) and run at 850 °C for 3 months gave an 80–85% yield. The dimensions of the phase depend somewhat on the loaded stoichiometry and/or the reaction period. The powder pattern of this compound looked identical to that of cubic Na_{0.5}Zr₆Cl₁₅C²¹ (*Ia*3̄*d*, stuffed Ta₆Cl₁₅ type²²) except that the diffraction lines were shifted to higher angles and some line intensities had changed. Sodium contents higher than that of NaHf₆Cl₁₅B always resulted in a phase with a tetragonal structure that bears a subgroup relationship to the cubic phase (below).

One of numerous dark purple chunky crystals from the reaction with an overall NaHf₆Cl₁₄B stoichiometry was utilized for structural refinement. Weissenberg photos confirmed the body-centered-cubic lattice, and one octant of data was collected on the Rigaku diffractometer. The space group of Na_{0.5}Zr₆Cl₁₅C, *Ia*3̄*d*, was consistent with the diffraction data and was used in the refinement. Following the usual data reduction and absorption correction with ψ -scan data, all observed reflections ($I > 3\sigma(I)$) yielded $R_{av} = 5.3\%$. Isotropic refinement starting with the positional parameters of Na_{0.5}Zr₆Cl₁₅C as a model gave $R/R_w = 7.2/6.0\%$, and the anisotropic refinement smoothly converged at 5.3/4.3%. The occupancy of the Na (48g) position refined to 0.27(7)% which, with $Z = 16$, yields an empirical formula of Na_{0.8(2)}Hf₆Cl₁₅B. The peak heights for the first five peaks in the final difference Fourier map ranged between 2.3 and 2.1 e/Å³, and the most negative peak was -2.3 e/Å³; in other words, nothing stood out from background. We were not able to synthesize any of this compound without sodium present. The refined positional and isotropic-equivalent thermal parameters are listed in Table 2.

Tetragonal Na_{0.8}Hf₆Cl₁₅B. As in the analogous zirconium system,²¹ a tetragonal phase that is also not a line phase is formed in reactions with higher Na contents. Diffraction data were collected on a Rigaku AFC6R diffractometer from a dark purple cylindrical crystal isolated after reaction of an Na₂Hf₆Cl₁₅B composition. Space group *I*4₁/*acd* was chosen on the basis of the systematic absences, and all observed data averaged $R_{av} = 8.5\%$ after absorption corrections based on ψ -scan measurements. The initial model provided by the direct methods package in SHELXS-86²³ contained all correct Hf and Cl positions. A

(21) Ziebarth, R. P.; Corbett, J. D. *J. Less-Common Met.* **1988**, *137*, 21.(22) Bauer, D.; von Schnering, H.-G. *Z. Anorg. Allg. Chem.* **1968**, *361*, 259.

Table 2. Positional and Thermal Parameters for Cubic $\text{Na}_{0.8(2)}\text{Hf}_6\text{Cl}_{15}\text{B}$

atom	x	y	z	$B_{\text{eq}} (\text{\AA}^2)^a$
Hf	0.06151(5)	0.96550(6)	0.07993(5)	1.77(5)
Cl1	0.1561(3)	0.0296(3)	0.0496(6)	2.4(3)
Cl2	0.1100(4)	0.8774(3)	0.0185(3)	2.5(3)
Cl3	0.5713(3)	$1/4 - x$	$1/8$	3.2(3)
Na^b	0.251(3)	$1/4 - x$	$1/8$	5(3)
B	0	0	0	0.4(10)

^a $B_{\text{eq}} = (8\pi^2/3)\sum_i\sum_j U_{ij}a_i^*a_j^*\bar{a}_i\bar{a}_j$. ^b Occupancy = 0.27(7).

fractional Na1 atom was located in a 32g position in a different Fourier map and then Na2 in 16f, as in the zirconium case (below). Their simultaneous isotropic refinement (TEXSAN) give ~0.65 (6) total sodium atoms per cluster but with apparent coupling between the B's (1 and 7 \AA^2 , respectively), so both were fixed at $B = 5$ and only the sodium positions and occupancies refined along with all of the heavy atoms anisotropically. The resulting composition was $\text{Na}_{0.76(6)}\text{Hf}_6\text{Cl}_{15}\text{B}$. The difference map showed peaks up to 2.3 $e/\text{\AA}^3$, with nothing else distinctive. The small values of B_{eq} refined for boron in both hafnium results are probably of no particular significance and arise because of both the other much heavier atoms and the fact that both interstitials lie at points of highest symmetry.

Tetragonal $\text{Na}_x\text{Zr}_6\text{Cl}_{15}\text{B}$. Apparently related tetragonal distortions of the corresponding cubic sodium zirconium chloride carbide and boride with increasing sodium content were observed earlier, but the nature of the structural change was not investigated.²¹ Therefore, reactions with the stoichiometries $\text{Na}_x\text{Zr}_6\text{Cl}_{15}\text{B}$, $x = 0.5, 1.0, 1.5, 2.0$, were carried out within an 866–824 °C temperature gradient for 30 days. In contrast to the behavior of the hafnium system (above), orthorhombic $\text{NaZr}_6\text{Cl}_{14}\text{B}$ was the only cluster phase formed in the first two reactions, while the target tetragonal phase was the major product in the third reaction and the only cluster phase in the last. The singularity of one of many dark red to purple crystals from the last was checked with an oscillation photograph, and one octant of diffraction data was collected with the aid of a CAD4 diffractometer in an ω -scan mode. The systematic absences and a statistical analysis again indicated space group $I4_1/acd$, and R_w was 4.3% for all observed data after absorption corrections based on ψ -scans. The initial model again provided by direct methods gave all Zr and Cl atoms as well as the interstitial B. In this case, two Na positions were subsequently located in a different Fourier map. Their positions, occupancies, and B's could all be reasonably refined in the presence of the lighter Zr, and this yielded $\text{Na}_{1.04(5)}\text{Zr}_6\text{Cl}_{15}\text{B}$ as the empirical formula. A difference Fourier map showed maximum differences of +1.8 and -1.1 $e\text{\AA}^{-3}$. The positional data for both tetragonal phases are listed in Table 3.

Results and Discussion

A large variety of Hf–HfCl₄ reactions have been examined in the presence of potential interstitial Z, namely for Be, B, C, Si, Mn, Fe, Ru, Os, or Ir, and with or without added AlCl_3 , $\text{A} = \text{Li–Cs, Ca–Ba}$. The hafnium cluster products found are relatively few compared with the great diversity known in the analogous zirconium systems, but they still amount to eleven new phases spanning four structure types. All the structures had been previously recognized, and most had been structurally defined. Hafnium examples were characterized for the following types: orthorhombic $\text{A}^1\text{Hf}_6\text{Cl}_{14}\text{Z}$ ($\text{CsZr}_6\text{I}_{14}\text{C}$,²⁴ $\text{LiZr}_6\text{Cl}_{14}\text{B}$,⁶ or $\text{Zr}_6\text{Cl}_{14}\text{C}$ ²⁵ variations), orthorhombic $\text{A}^1\text{Hf}_6\text{Cl}_{15}\text{C}$ ($\text{KZr}_6\text{Cl}_{15}\text{C}$ ²⁶ and $\text{CsNb}_6\text{Cl}_{15}$ ²⁷ types), cubic $\text{Na}_{0.8}\text{Hf}_6\text{Cl}_{15}\text{B}$ ($\text{Na}_{0.5}\text{Zr}_6\text{Cl}_{15}\text{C}$ ²¹), and the related tetragonal $\text{Na}_{0.8}\text{Hf}_6\text{Cl}_{15}\text{B}$ and $\text{NaZr}_6\text{Cl}_{15}\text{B}$ (new). There was no sign of $\text{Hf}_6\text{Cl}_{12}\text{Z}$ or $\text{A}_x\text{Hf}_6\text{Cl}_{18}\text{Z}$ type phases, in contrast to the analogous zirconium systems. Only the small B and C appeared to be effective as interstitials

Table 3. Positional and Thermal Parameters for Tetragonal $\text{Na}_{0.76(6)}\text{Hf}_6\text{Cl}_{15}\text{B}$ and $\text{Na}_{1.04(5)}\text{Zr}_6\text{Cl}_{15}\text{B}^a$

atom	x	y	z	$B_{\text{eq}} (\text{\AA}^2)^b$
$\text{Na}_{0.76(6)}\text{Hf}_6\text{Cl}_{15}\text{B}$				
Hf1	0.42116(6)	0.06070(6)	0.03419(6)	2.38(7)
Hf2	0.56048(7)	0.03457(7)	0.07964(5)	2.31(6)
Hf3	0.32856(6)	0.21563(7)	0.31134(6)	2.26(6)
Cl1	0.2691(4)	0.1275(4)	0.3597(3)	2.5(4)
Cl2	0.4805(4)	0.1087(4)	0.1231(3)	2.8(4)
Cl3	0.0494(4)	0.1559(4)	0.0304(4)	3.3(4)
Cl4	0.0288(4)	0.0488(4)	0.1562(3)	2.6(4)
Cl5	0.3227(4)	0.1249(5)	0.0717(4)	4.6(5)
Cl6	0.1552(4)	0.0292(5)	0.0504(4)	3.8(5)
Cl7	0.0715(4)	$x + 1/4$	$1/8$	3.6(3)
Cl8	0.6083(4)	0.1226(4)	0.0187(3)	3.1(4)
$\text{Na}1^c$	0.624(3)	0.248(3)	0.002(2)	5.0
$\text{Na}2^d$	0.251(4)	$x + 1/4$	$1/8$	5.0
B	0	0	0	0.4(6)
$\text{Na}_{1.04(5)}\text{Zr}_6\text{Cl}_{15}\text{B}$				
Zr1	0.4206(1)	0.0611(7)	0.0347(1)	2.5(1)
Zr2	0.5613(1)	0.0344(1)	0.07890(9)	2.6(1)
Zr3	0.3298(1)	0.2154(1)	0.31039(9)	2.7(1)
Cl1	0.2685(3)	0.1271(3)	0.3576(3)	4.4(3)
Cl2	0.4817(3)	0.1081(3)	0.1222(3)	4.2(3)
Cl3	0.0496(3)	0.1558(3)	0.0282(3)	4.4(3)
Cl4	0.0297(3)	0.0503(3)	0.1544(2)	4.8(4)
Cl5	0.3213(3)	0.1245(4)	0.0722(3)	5.6(4)
Cl6	0.1561(3)	0.0292(3)	0.0487(3)	4.5(3)
Cl7	0.0713(3)	$x + 1/4$	$1/8$	6.8(4)
Cl8	0.6085(3)	0.1226(3)	0.0185(2)	4.0(3)
$\text{Na}1^e$	0.624(2)	0.249(2)	0.002(1)	6(1)
$\text{Na}2^f$	0.249(1)	$x + 1/4$	$1/8$	5(1)
B	0	0	0	2.2(6)

^a Origins at $\bar{1}$. ^b $B_{\text{eq}} = (8\pi^2/3)\sum_i\sum_j U_{ij}a_i^*a_j^*\bar{a}_i\bar{a}_j$. ^c Occupancy = 0.27(3). ^d Occupancy = 0.21(4). ^e Occupancy = 0.34(2). ^f Occupancy = 0.36(3).

in the smaller hafnium clusters (nitrogen was not investigated). The foregoing types will be described separately.

$\text{M}_x\text{Hf}_6\text{Cl}_{14}\text{Z}$. Phases based on a stuffed $\text{Nb}_6\text{Cl}_{14}$ structure²⁸ are common and occur for many examples of $\text{Zr}_6\text{X}_{14}\text{Z}$. The intercluster connectivity is provided by two inner halogens from each M_6X_{12} unit that bridge to vertices of other clusters (X^{i-a}) as well as by two halogens beyond the basic 12 that bridge between cluster vertices, X^{a-a} . This is $[(\text{Zr}_6\text{Z})\text{X}^{i_0}\text{X}^{i-a/2}]\text{X}^{a-i/2}\text{X}^{a-a/2}$ more precisely expressed.

This investigation provided seven $\text{A}^1\text{Hf}_6\text{Cl}_{14}\text{Z}$ type phases in three variations, all of which represent various ways to stuff the $\text{Nb}_6\text{Cl}_{14}$ parent structure with an interstitial in each cluster and, in many cases, one alkali-metal cation per cluster within the halogen sublattice. These and their Guinier-based lattice parameters are compiled in Table 4. As seen, these hafnium chloride cluster phases have 1.6–2.9% smaller cell volumes than the corresponding zirconium members where both examples are known. The two quaternary types $\text{CsZr}_6\text{I}_{14}\text{C}$ and $\text{LiZr}_6\text{Cl}_{14}\text{B}$ differ only regarding in which cavity in the halide matrix a large 12-coordinate or small 6-coordinate countercation is placed, the latter being disordered over 4 times as many sites. Within $\text{A}^1\text{Zr}_6\text{Cl}_{14}\text{B}$ and $\text{A}^1\text{Zr}_6\text{Br}_{14}\text{C}$ series only Li occurs in the smaller site, as signalled by clearly smaller cell volumes for Na^+ and K^+ , respectively, while both Li^+ and Na^+ do so in the larger $\text{Zr}_6\text{Cl}_{14}\text{Mn}$ host.^{6,10} The cavities for A^1 must be smaller in $\text{Hf}_6\text{Cl}_{14}\text{B}$, and only $\text{LiHf}_6\text{Cl}_{14}\text{B}$ clearly falls in this category (type 1, Table 4), producing a larger cell than the salts of either Na^+ or K^+ which contract the larger site (type 2). (Some countervailing contraction from $\text{Hf}_6\text{Cl}_{14}\text{B}$ to $\text{LiHf}_6\text{Cl}_{14}\text{B}$ must follow from the fact that the former contains only 13 rather

(23) Sheldrick, G. M. SHELXS-86. Universität Göttingen, BRD, 1986.
 (24) Smith, J. D.; Corbett, J. D. *J. Am. Chem. Soc.* **1985**, *107*, 5704.
 (25) Ziebarth, R. P.; Corbett, J. D. *J. Solid State Chem.* **1989**, *80*, 56.
 (26) Ziebarth, R. P.; Corbett, J. D. *J. Am. Chem. Soc.* **1987**, *109*, 4844.
 (27) Imoto, H.; Simon, A. Unpublished research, 1980.

(28) Simon, A.; von Schnering, H.-G.; Wöhrle, H.; Schäfer, H. Z. *Anorg. Allg. Chem.* **1965**, *339*, 155.

Table 4. Cell Dimensions (Å) and Volume (Å³) of AHf₆Cl₁₄Z Phases and the Volume Changes from the Corresponding Zirconium Compounds (AZr₆Cl₁₄Z) (Space Group *Cmca*)

stoichiometry	<i>a</i>	<i>b</i>	<i>c</i>	<i>V</i>	cation site ^a	Δ <i>V</i> (%) ^b
Hf ₆ Cl ₁₄ B	14.014(2)	12.576(2)	11.602(3)	2044.7(6)		-1.63
LiHf ₆ Cl ₁₄ B	14.162(1)	12.574(2)	11.426(3)	2034.8(4)	1	-2.24
NaHf ₆ Cl ₁₄ B	13.985(1)	12.530(2)	11.416(2)	2000.6(4)	2	-2.86
KHf ₆ Cl ₁₄ B	13.9718(9)	12.5456(8)	11.4603(7)	2008.8(2)	2	-2.54
Hf ₆ Cl ₁₄ C	13.938(2)	12.498(3)	11.399(2)	1985.7(7)		-1.79
LiHf ₆ Cl ₁₄ C	13.887(1)	12.484(1)	11.356(1)	1968.7(3)	2	
NaHf ₆ Cl ₁₄ C	13.904(2)	12.475(2)	11.370(2)	1972.2(5)	2	

^a 1, the 6-coordinate Li position in LiZr₆Cl₁₄Mn;⁶ 2, that of 12-coordinate Cs in CsZr₆I₁₄C.⁸ ^b Δ*V*(%) = 100[V(AHf₆Cl₁₅C) - V(AZr₆Cl₁₅C)]/V(AZr₆Cl₁₅C).

Table 5. Cell Data (Å, Å³) for Orthorhombic AHf₆Cl₁₅C Phases (*Pmma*)

	<i>a</i>	<i>b</i>	<i>c</i>	<i>V</i>	cation site ^a	Δ <i>V</i> (%) ^b
KHf ₆ Cl ₁₅ C	18.289(3)	13.866(3)	9.603(2)	2435.8(8)	1	-2.2
CsHf ₆ Cl ₁₅ C	18.369(2)	13.818(2)	9.573(3)	2429.9(9)	2	-2.2

^a Based on powder pattern intensities. 1 and 2 are the K and Cs positions, respectively, in CsKZr₆Cl₁₅B.²⁶ ^b Δ*V*(%) = 100[V(Hf) - V(Zr)]/V(Zr).

Table 6. Important Bond Distances (Å) in Cubic Na_{0.8(2)}Hf₆Cl₁₅B

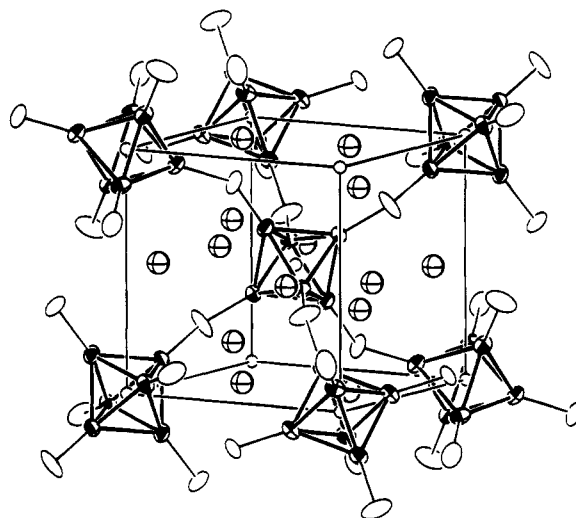
Hf-2Hf	3.225(2)	Na-2Cl1	2.69(6)
	3.235(2)	Na-2Cl2	2.74(7)
\bar{d}	3.230	Na-2Cl3	3.30(2)
		\bar{d} (CN=4)	2.72
Hf-B	2.284(1)		
Hf-Cl1 ⁱ	2.525(7)		
	2.533(7)	Cl1-Cl2 ^a	3.47(1)
Hf-Cl2 ⁱ	2.525(7)	Cl1-Cl3	3.336(8)
	2.528(7)	Cl2-Cl2	3.36(1)
Hf-Cl3 ^{a-a}	2.636(4)	Cl2-Cl3	3.403(9)

^a *d*(Cl-Cl) < 3.54 Å.

than the optimal 14 cluster-based electrons.) The AHf₆Cl₁₄C lattices, the smallest known in this structure type, seem noteworthy in that Li⁺ and Na⁺ appear to occupy the same, probably 12-coordinate, site judging from their cell volumes, especially that *V*_{Li} < *V*_{Na} < *V*_{empty} even though the first two are 15-electron clusters. The two types cannot be distinguished by powder pattern intensities for the lighter A.

AHf₆Cl₁₅C. Two orthorhombic phases with this stoichiometry, KHf₆Cl₁₅C and CsZr₆Cl₁₅C, were synthesized during this investigation and characterized by powder data, Table 5. They both have the structural framework first identified in CsNb₆Cl₁₅²⁷ (which lacks the interstitial), namely a connectivity [M₆Cl₁₂]Cl^{a-a}_{6/2}. There are several ways to achieve such networks with this connectivity, and this particular structure contains perpendicular, interbridged zig-zag and linear chains of clusters in which two different sized cation sites have been identified in KZr₆Cl₁₅C and in CsKZr₆Cl₁₅B where both are occupied.²⁶ Which is occupied can be readily deduced from intensities of powder diffraction data for the heavier alkali metals. The dispositions of cations in the hafnium phases parallel those for the corresponding zirconium compounds. The hafnium cell volumes are both 2.2% less, and the nonuniform contractions of cell dimensions indicate some angular changes in cluster bridging must also accompany the change in cluster metals.

Cubic Na_{0.8(2)}Hf₆Cl₁₅B. This phase is isostructural with Na_{0.53(3)}Zr₆Cl₁₅C,²¹ which adopts a different bridged cluster network than just discussed, one that was first identified for Ta₆Cl₁₅.²² The heavier hafnium clearly makes the refinement of the fractional sodium content less precise. Figure 1 shows the nominal body-centered-cubic arrangement of interconnected [Hf₆(B)Cl₁₂]Cl^{a-a}_{6/2} cluster units that are present (in different

**Figure 1.** One-eighth of the unit cell of Na_{0.8}Hf₆Cl₁₅B with one of the 3-fold axes (*1a3d*). The 90% ellipsoids are open, Cl, shaded, Hf, crossed, Na (~27% occupied). Only the intercluster bridging chlorine (Cl^{a-a}) atoms are shown for clarity.

orientations) in each octant of the cell. The complete cell is rather complex with seven nonintersecting 3-fold axes like the one shown that generate a ccp array of clusters ..(ABC)₄.. along the unique [111] axis.²¹

The individual cluster units here have a nearly ideal *O_h* with about a 3.5σ elongation along the $\bar{3}$ axis. Although the ideal 14-electron cluster is achieved in the isostructural Zr₆Cl₁₅N (the hafnium example was not investigated), this lattice evidently has insufficient room or "give" to accommodate one full sodium ion per cluster (or any larger ions) with earlier Z, and so the two examples are both electron-poor, Na_{0.53(3)}Zr₆Cl₁₅C and Na_{0.8(2)}Hf₆Cl₁₅B. The cations are distributed fractionally over a 48g site which places them in pairs on the faces of the cell octants, at 27(7)% occupancy in the present case. The cation appears to have a somewhat unfavorable environment, 4Cl at ~2.72 Å in a distorted tetrahedron with two more relatively distant chlorines at 3.30 Å (Table 6). The sum of the crystal radii for CN4²⁹ is 2.80 Å, which would be most meaningful for full site occupancy. Because of the interstitial change from carbon to boron, the present Na_{0.8(2)}Hf₆Cl₁₅B is appreciably electron poorer than is Na_{0.53(3)}Zr₆Cl₁₅C. The hafnium carbide was not achieved, perhaps because the smaller cluster would leave even less room for sodium. Nonetheless, attempts to achieve electron-richer examples of either cubic phase by reacting more sodium always produced the following tetragonally-distorted phases, so the stability must be limited principally by the number of cations that can be accommodated.

Tetragonal Na_{0.76(6)}Hf₆Cl₁₅B. The framework of this tetragonal phase is very similar to that of the cubic one, and the

(29) Shannon, R. P. *Acta Crystallogr.* 1976, A32, 751.

Table 7. Cell Dimensions (Å, Å³) of Cubic and Tetragonal Na_xHf₆Cl₁₅B Products of Different Reactions^a

stoichiometry loaded	<i>a</i>	<i>c</i>	<i>c/a</i>	<i>V</i>
NaHf ₆ Cl ₁₄ B ^b	21.428(2)			9839(3)
NaHf ₆ Cl ₁₅ B	21.3560(8)			9740(1)
Na _{0.8} Hf ₆ Cl ₁₅ B	21.356(1)			9740(2)
Na ₂ Hf ₆ Cl ₁₅ B ^b	21.540(2)	21.387(3)	0.9929	9923(2)
Na ₂ Hf ₆ Cl ₁₅ B	21.543(2)	21.378(3)	0.9923	9922(2)
Na _{1.5} Hf ₆ Cl ₁₅ B	21.524(2)	21.342(2)	0.9915	9887(1)

^a 850 °C; 60–80% yields. ^b Source of single crystals for diffraction studies.

Table 8. Interatomic Distances (Å) in Tetragonal Na_{0.76(6)}Hf₆Cl₁₅B and Na_{1.04(5)}Zr₆Cl₁₅B

	Hf	Zr		Hf	Zr
M1–M2	3.204(2)	3.243(3)	Na1–Cl2	2.72(5)	2.81(3)
	3.209(2)	3.247(3)	Na1–Cl3	2.72(6)	2.69(3)
M1–M3	3.202(2)	3.245(3)	Na1–Cl4	2.72(6)	2.75(3)
	3.206(2)	3.245(3)	Na1–Cl8	2.75(6)	2.79(4)
M2–M3	3.204(2)	3.242(3)	Na1–Cl5	3.32(6)	3.35(3)
	3.211(2)	3.248(3)	Na1–2Cl7	3.30(6)	3.35(3)
<i>d</i>	3.206	3.245			
M1–B	2.265(1)	2.295(2)	Na2–2Cl11	2.83(5)	2.77(3)
M2–B	2.270(1)	2.295(2)	Na2–2Cl6	2.64(7)	2.73(3)
M3–B	2.267(1)	2.294(2)	Na2–2Cl5	3.32(5)	3.32(1)
<i>d</i>	2.267	2.295			
<i>d</i> (M–Cl ^l)			Cl1–Cl1 ^a	3.37(1)	3.41(1)
M1–Cl1	2.538(7)	2.524(6)	Cl1–Cl4	3.47(1)	3.52(1)
M1–Cl2	2.512(7)	2.533(6)	Cl1–Cl5	3.42(1)	3.41(1)
M1–Cl3	2.552(8)	2.547(6)	Cl2–Cl3	3.49(1)	3.501(9)
M1–Cl6	2.537(8)	2.556(6)	Cl2–Cl5	3.42(1)	3.431(9)
M2–Cl2	2.526(8)	2.528(6)	Cl2–Cl8	3.36(1)	3.431(8)
M2–Cl4	2.524(7)	2.554(6)	Cl3–Cl7	3.33(1)	3.395(8)
M2–Cl6	2.538(8)	2.555(7)	Cl4–Cl5	3.37(1)	3.387(9)
M2–Cl8	2.520(8)	2.533(6)	Cl5–Cl6	3.36(1)	3.380(9)
M3–Cl1	2.512(8)	2.541(7)	Cl6–Cl8	3.49(1)	3.50(1)
M3–Cl3	2.543(8)	2.551(6)	Cl7–2Cl8	3.395(9)	3.450(7)
M3–Cl4	2.523(6)	2.556(6)			
M3–Cl8	2.524(7)	2.524(6)			
<i>d</i> (M–Cl ^{a-a})					
M1–Cl5	2.655(8)	2.674(6)			
M2–Cl5	2.659(8)	2.686(6)			
M3–Cl7	2.669(5)	2.682(4)			

^a *d*(Cl–Cl) < 3.54 Å.

major (but still subtle) differences appear to be in the Na positions. The 48-fold site in the cubic structure splits into 32- and 16-fold positions in the tetragonal lattice, and both are partially occupied (about 27 and 21%, respectively). At face value, the sodium contents of cubic Na_{0.8(2)}Hf₆Cl₁₅B and tetragonal Na_{0.76(6)}Hf₆Cl₁₅B are the same. However, both synthetic evidence and the cell volumes listed in Table 7 for a number of reactions clearly indicate that the tetragonal phase has a higher Na content; both are probably somewhat nonstoichiometric as well. The relatively large errors on the refined Na occupancies disguise the subtle, yet indispensable, difference in sodium in these two structure types.

Two changes may reflect the driving force for the transformation from cubic to tetragonal symmetry. The average Hf–Hf distance, 3.205 Å (and the geometrically related *d*(Hf–B), Table 8), in the latter is 0.025 Å less than in the cubic phase, the point symmetry changing from $\bar{3}$ to $\bar{1}$. The Hf–Cl^{a-a} bridging distances reasonably change in the opposite sense, increasing by 0.02 Å, presumably to afford more intercluster room. In addition, Na1 gains one more secondary chlorine neighbor at ~3.30 Å in addition to the four near 2.73 Å. The dimensional errors are too large to say whether there are significant near-neighbor distance changes within each sodium environment. Although close Cl^l••Cl contacts appear to increase (Tables 6

and 8), their averages are virtually the same, and the increase in frequency is just that in the decrease in atom multiplicities.

There are six “layers” of Na atoms along \bar{a} and \bar{b} , and only four in the \bar{c} direction, consistent with the tetragonal axis along the latter. The increased sodium content thus produces a smaller cluster, slightly larger Hf–Cl^{a-a} distances and perhaps some improved bonding of the sodium. The transition is probably continuous (second order).

Tetragonal Na_{1.04(5)}Zr₆Cl₁₅B. The earlier study of the nominally isovalent and isostructural series Zr₆Cl₁₅N, NaZr₆Cl₁₅C, and Na₂Zr₆Cl₁₅B revealed that the product of the second reaction was cubic and substoichiometric in Na (0.53(3)) while the phase formed in the third was evidently tetragonal (*a* = 21.603(5) Å, *c* = 21.763(9) Å from the diffractometer).²¹ The structure determination was not pursued at that time. Since that cubic-tetragonal distortion is in fact in the opposite direction from that found with hafnium, it was considered worthwhile to characterize the tetragonal zirconium phase structurally as well.

The cluster again is nearly octahedral, and the Zr–B distance, 2.295 Å, about 0.03 Å longer than Hf–B (Table 8). On the other hand, *d*(Zr–B) at 2.295(2) Å is still somewhat less than seen before,³⁰ including in phases with the same 6–15 stoichiometry and general connectivity but with more open structures and larger cations (K₂Zr₆Cl₁₅B, 2.304 Å,³¹ CsKZr₆Cl₁₅B, 2.307 Å²⁶ average) and 14- rather than 13-cluster electrons as well. The exo Zr–Cl^{a-a} distances likewise average 0.04–0.06 Å longer than seen before, an opposed change that seems appropriate for binding a few relatively small cations in this tightly packed network structure.³²

Interestingly, the direction of the tetragonal distortion for the zirconium phase is opposite (*c/a* > 1) to that with the smaller hafnium cluster. Both the same 32- and 16-fold split cation sites are again fractionally occupied, by 34(2) and 36(3)% Na, respectively. The first cation has a somewhat more distorted first neighbor environment than with hafnium, but it again gains one more distant anion neighbor relative to the cubic Na_{0.53}-Zr₆Cl₁₅C (*d*(Na–Cl) = 2.71(3), 2.73(2), and 3.32(3) Å, each twice²¹) while Na2 has effectively the same environment as without distortion. Changes in M–Cl^l distances (Table 8) clearly reflect the opposite sense of the distortions. Only differences in size of the Hf₆(B)Cl₁₂ vs Zr₆(B)Cl₁₂ building blocks appear to be significant regarding the opposed changes, although the problem in detail is probably rather complex. The Cl^l••Cl separations are also larger with zirconium, as expected.

The cubic Na_{0.8(2)}Hf₆Cl₁₅B and tetragonal Na_{0.76(6)}Hf₆Cl₁₅B phases have about 12.8 cluster-based electrons, and each exhibits paramagnetic, Curie–Weiss properties above about 100 K that correspond to effective moments of 1.54(2) μ_B and 1.68(3) μ_B , respectively. A *t*_{2g}⁵ HOMO would be expected for a 13-electron cluster on the basis of extended Hückel calculations on zirconium clusters.¹ The results are slightly lower than expected for 13 electrons but consistent considering the moderate-sized compositional uncertainties. The susceptibilities increase appreciably at lower temperatures and also slightly at the higher temperatures (relative to Curie–Weiss). Significant spin–orbital coupling by hafnium may also be present, so the deviations from the simplest picture are probably not meaningful.

We have also incompletely characterized a monoclinic (C2/c) Li_xHf₆Cl₁₆B with squarish layers, somewhat similar to those

(30) Ziebarth, R. P.; Corbett, J. D. *J. Am. Chem. Soc.* **1989**, *111*, 3272.

(31) Ziebarth, R. P.; Corbett, J. D. *J. Am. Chem. Soc.* **1988**, *110*, 1132.

(32) Corbett, J. D. In *Modern Perspectives in Inorganic Crystal Chemistry*; Parthé, E., Ed.; Kluwer Academic Publishers: Dordrecht, The Netherlands, 1992; p 27.

in orthorhombic $\text{Na}_4\text{Zr}_6\text{Cl}_{16}\text{Be}$.³³ The lithium number (~ 3) and location could not be well-defined. The two most reasonable cavities are general positions, so some fractional occupancies would be expected as well. The carbide also exists.

Acknowledgment. The authors are indebted to R. A. Jacobson and V. Young for provision of the diffractometers and to J. E. Ostenson and D. K. Finnemore for the magnetic data.

(33) Ziebarth, R. P.; Corbett, J. D. *Inorg. Chem.* **1989**, *28*, 626.

This research was supported by the National Science Foundation, Solid State Chemistry, via Grants DMR-8902954 and DMR-9207361 and was carried out in facilities of the Ames Laboratory, DOE.

Supplementary Material Available: Tables of additional collection and refinement parameters and of anisotropic displacement parameters for the three structures (S1–S4) (3 pages). Ordering information is given on any current masthead page.